Preparation, Crystal and Magnetic Structure of the Double Perovskites Ca_2TWO_6 (T = Co, Ni)

M. J. Martínez-Lope[a], J. A. Alonso[a], M. T. Casais[a], and M. T. Fernández-Díaz[b]

[a] Instituto de Ciencia de Materiales de Madrid, C.S.I.C., Cantoblanco, E-28049 Madrid, Spain
[b] Institut Laue-Langevin, B.P. 156, F-38042 Grenoble Cedex 9, France

Reprint requests to Dr. J. A. Alonso. E-mail: ja.alonso@icmm.csic.es

Z. Naturforsch. **58b,** 127 – 132 (2003); received September 6, 2002

Ca_2TWO_6 (T = Co, Ni) perovskites have been prepared in polycrystalline form by thermal treatment, in air, of previously decomposed citrate precursors. These materials have been studied by X-ray (XRD) and neutron powder diffraction (NPD) data. Our results show that these compounds crystallize, at room temperature, in the monoclinic space group $P2_1/n$. The two perovskites contain divalent T (T = Co, Ni) cations. The low temperature antiferromagnetic ordering has been followed from sequential NPD data. Peaks of magnetic origin appear at the NPD patterns below temperatures of T_N = 36 K and T_N = 56 K for the Co and Ni compounds, respectively. The magnetic structures are both defined by a propagation vector **k** = (1/2, 0, 1/2), and can be described as an array of ferromagnetic layers of Co(Ni) moments, perpendicular to the [101] directions, coupled antiferromagnetically.

Key words: Perovskites, X-Ray Data

Introduction

The recent discovery of colossal magnetoresistance (CMR) in perovskite manganites [1 – 3] and its potential applications have stimulated the search for new magnetoresistive ferromagnetic metallic oxides. CMR materials undergo a large change in electrical resistance in response to an external magnetic field. In these compounds, the applied field tends to align the local spins and hence leads to a rapid drop of the measured resistivity by suppressing spin fluctuations and enhancing electronic transfer.

Much of the present interest in double perovskite oxides arises from the prospects of finding half-metallic materials with high Curie temperatures (T_C). More than 300 compounds with double-perovskite structure, $A_2B'B''O_6$, have been synthesized [4], in which the perovskite B sites are occupied alternately by different cations B' and B''. Among them, A_2FeMoO_6 (A = Ca, Sr, and Ba) are known to be ferromagnetic with critical temperature T_C ($\cong$ 330 – 420 K) [5], which is higher than that of the doped manganites (maximum T_C is $\cong$ 360 K for $La_{0.4}Sr_{0.6}$ MnO_3). Kobayashi *et al.* [6, 7] have observed room temperature magnetoresistance in Sr_2FeMoO_6 and Sr_2FeReO_6 due to intergrain tunneling [6 – 10]. These results have expanded the options for optimizing CMR properties for specific technological applications, and led to search in other members of the wide family of perovskites of composition $A_2B'B''O_6$ (A = alkali earths, B' and B'': transition metals).

The double perovskites Ca_2CoWO_6 and Ca_2NiWO_6 have attracted our attention. They were studied in the sixties and forgotten for more than 30 years. The crystal structures of Ca_2NiWO_6 and Ca_2CoWO_6 have been described as orthorhombic [11]. An antiferromagnetic behavior was observed for Ca_2CoWO_6 below T_N = 26 K [12].

In the present work we describe the synthesis of Ca_2TWO_6 (T = Co, Ni), prepared by soft chemistry procedures, and the results of a neutron powder diffraction study on well-crystallized samples. The crystal structures have been revisited; we report complete structural data for these monoclinic perovskites. Low temperature NPD data allowed us to probe the microscopic origin of the antiferromagnetic ordering, concerning the Co^{2+} and Ni^{2+} magnetic moments.

Experimental Section

Ca_2TWO_6 (T = Co, Ni) perovskites were prepared as brown (T = Co) or green (T = Ni) polycrystalline powders from citrate precursors obtained by soft chemistry procedures. Stoichiometric amounts of analytical grade $CaCO_3$, $H_{26}N_6O_{41}W_{12} \cdot 18\ H_2O$, $Co(NO_3)_2 \cdot 6\ H_2O$ or $Ni(NO_3)_2 \cdot 6\ H_2O$, were dissolved in citric acid. The citrate / nitrate solu-

tions were slowly evaporated, leading to organic resins with a random distribution of the involved cations at an atomic level. These resins were first dried at 120 °C and then slowly decomposed at temperatures up to 600 °C. All the organic materials and nitrates were eliminated in a subsequent treatment at 800 °C in air, for 2 h. This treatment gave rise to highly reactive precursor materials. Afterwards, the resulting brown or green powders were treated at 1100 °C in air for 12 h.

The initial characterization of the products was carried out by laboratory X-ray diffraction (XRD) (Cu $K_\alpha, \lambda =$ 1.5406 Å). Neutron powder diffraction (NPD) diagrams were collected at the Institut Laue-Langevin (ILL) in Grenoble (France). The crystallographic structures were refined from the high resolution NPD patterns, acquired at room temperature at the D2B diffractometer with λ = 1.594 Å. For the determination of the magnetic structures and the study of their thermal variation, a series of NPD patterns was obtained at the D20 high-flux diffractometer (ILL-Grenoble) with a wavelength of 2.42 Å, in the temperature range from 2 to 82 K for T = Co and 2 to 90 K for T = Ni. The refinements of both crystal and magnetic structures were performed by the Rietveld method, using the FULLPROF refinement program [13]. A pseudo-Voigt function was chosen to generate the line shape of the diffraction peaks. The following parameters were refined in the final runs: scale factor, background coefficients, zero-point error, pseudo-Voigt corrected for asymmetry parameters, positional coordinates, isotropic thermal factors, anti-site disorder of Co(Ni)/W and O occupancies. The coherent scattering lengths for Ca, Co, Ni, W and O were 4.70, 2.49, 10.30, 4.86, and 5.803 fm, respectively.

Results

Ca_2TWO_6 (T = Co, Ni) were obtained as well crystallized powders; their XRD diagrams are shown in Figure 1. The patterns are characteristic of perovskite-type structures, showing superstructure peaks (with odd indices) corresponding to the T/W (T = Co, Ni) ordering. Minor amounts of $CaWO_4$ were detected from either XRD or NPD data; the main reflections of the impurity are indicated with stars in Figure 1. A small amount of NiO was detected only in the NPD pattern of Ca_2NiWO_6.

Crystallographic Structure

The crystal structure refinement was performed from the D2B high resolution data collected at room temperature and with a wave-length $\lambda = 1.594$ Å. In the two compounds the Bragg reflections were indexed with a monoclinic unit cell and the structures were refined in the monoclinic space group $P2_1/n$. $CaWO_4$

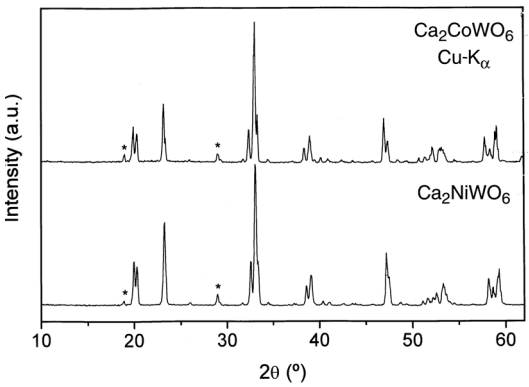

Fig. 1. XRD patterns for Ca_2TWO_6 (T = Co, Ni). The stars indicate the main reflections of the $CaWO_4$ impurity phase.

and NiO were included as secondary phases in the final refinement (NiO only for Ca_2NiWO_6). $CaWO_4$ is tetragonal (space group $I4_1/a$). From the scale factors of the main and secondary phases, we estimated 5% of $CaWO_4$ in Ca_2CoWO_6; 6% of $CaWO_4$ and 0.5% of NiO in Ca_2NiWO_6. In the final refinement, the possibility of anti-site disordering was also checked, by assuming that some Co(Ni) atoms could occupy W sites, and vice-versa: the refinement of the inversion degree led to less than 1% of anti-site disordering. The oxygen stoichiometry of O1, O2, and O3 was also checked by refining their occupancy factors; no oxygen vacancies were found within the standard deviations. The good agreement between the observed and calculated patterns after the refinement is shown in Figure 2. The lattice parameters and the final atomic coordinates of the different compounds are reported in Table 1. The mean interatomic distances and some selected bond angles are listed in Table 2. A drawing of the structure is shown in Figure 3. The perovskite structure is fairly distorted due to the small size of the Ca^{2+} cations, which force the Co(Ni)O_6 and WO_6 octahedra to tilt in order to optimize the Ca—O bond distances. Co(Ni)O_6 and WO_6 octahedra are fully ordered and alternate along the three directions of the crystal, in such a way that each Co(Ni)O_6 octahedron is linked to 6 WO_6 octahedra, as shown in Fig. 3, and vice-versa. The structure, thus, contains alternating Co(Ni)O_6 and WO_6 octahedra, tilted in phase along the (100) direction of the pseudocubic cell and in anti-phase along the (010) and (001) directions, which corresponds to the $a^+b^-b^-$ Glazer's notation as derived by Woodward [14] for 1 : 1 ordering in double perovskites, consistent with space group $P2_1/n$.

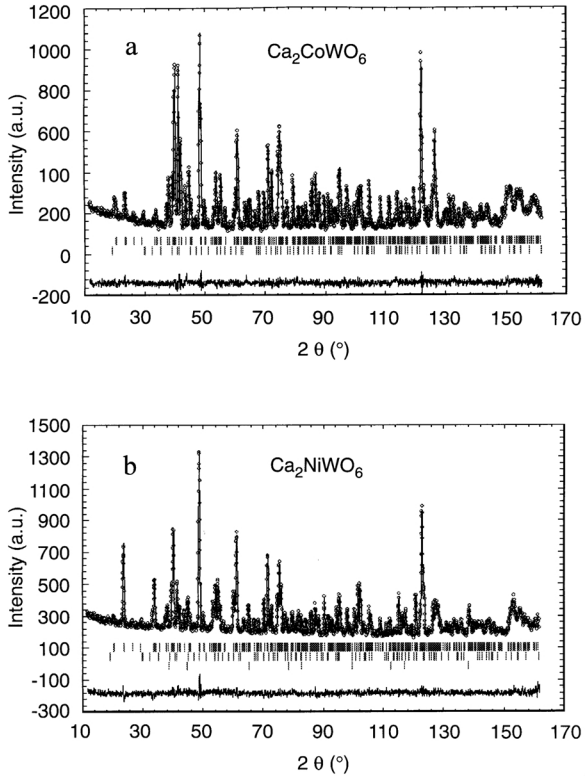

Fig. 2. Observed (crosses), calculated (full line) and difference (bottom) NPD Rietveld profiles for Ca_2TWO_6 at 298 K. Vertical lines correspond to the Bragg positions for the perovskites (top series) and minor impurity phases (bottom series). (a) T = Co; (b) T = Ni.

In both Ca_2CoWO_6 and Ca_2NiWO_6 unit cells, the monoclinic distortion is very small, with β angles very close to 90°; this effect has been observed in many 1 : 1 ordered perovskites with a strong pseudo-orthorhombic character. The size of the unit cell is larger for Ca_2CoWO_6 as expected for the larger Co^{2+} ionic radius (0.745 Å) *versus* Ni^{2+} (0.69 Å) in octahedral coordination [15]. The average ⟨T—O⟩ interatomic distances (Table 2, Co—O: 2.093(2) Å *vs.* Ni—O: 2.066(3) Å) are also in agreement with the larger size of the Co^{2+} cations.

Magnetic Structure

The magnetic structure for Ca_2TWO_6 (T = Co, Ni) and its thermal evolution were analyzed from a set of NPD patterns collected in the temperature range $2 < T < 82$ K for T = Co and $2 < T < 90$ K for T = Ni, with λ = 2.42 Å. In Ca_2CoWO_6, upon decreasing of the temperature below 36 K, new reflections appear

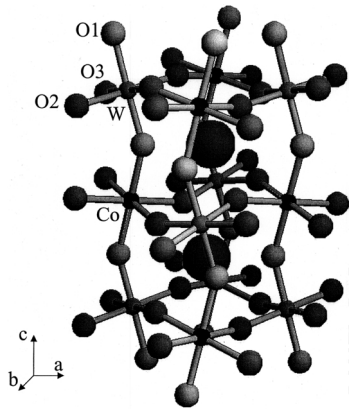

Fig. 3. View of the structure of monoclinic Ca_2CoWO_6 at 298 K. **c** axis is vertical; **a** axis from left to right. Large spheres represent Ca; small spheres represent O; corner-sharing CoO_6 and WO_6 octahedra are tilted in order to optimize Ca-O bond-lengths.

on positions forbidden for the Bragg crystallographic reflections in the space group $P2_1/n$. These new peaks correspond to magnetic satellites defined by the propagation vector **k** = (1/2, 0, 1/2). An antiferromagnetic structure was modeled with magnetic moments at the Co positions; after the full refinement of the profile, including the magnetic moment magnitude, a discrepancy factor of R_{mag} = 6.70% was reached for the 2 K diagram, collected with a good counting statistics. In Ca_2NiWO_6 the new peaks appear below T_N = 56 K and are also indexed with the same propagation vector **k** = (1/2, 0, 1/2). After the refinement of the antiferromagnetic structure, a discrepancy factor of R_{mag} = 5.77% was obtained for the 2 K diagram.

The best agreement was obtained by considering the magnetic moments aligned along the (011) directions. A view of the magnetic structure is displayed in Figure 4. The proposed magnetic arrangement gives rise to antiferromagnetic couplings between each Co(Ni) moment and the six nearest neighbors, *via* –O–W–O– paths. The magnetic structure can also be described as an array of ferromagnetic layers of Co(Ni) moments, perpendicular to the [101] directions, coupled antiferromagnetically. The magnetic structure is stable from 2 K to T_N, as demonstrated in a sequential refinement in all of the available temperature range. The thermal evolution of the ordered magnetic moment on the Co(Ni) positions is shown in Fig. 5. A sharp increase is observed below 36 K (T = Co) or 56 K (T = Ni), reaching the saturation value of 3.00(4) μ_B (T = Co) and 1.94(2) μ_B (T = Ni) at 2 K. These values

Table 1. Unit-Cell, positional and thermal parameters for Ca_2TWO_6 (T = Co, Ni) in the monoclinic $P2_1/n$ space group, from NPD data at 295 K.

		T = Co	T = Ni
a (Å)		5.42475(9)	5.4048(1)
b (Å)		5.57959(8)	5.5369(1)
c (Å)		7.7134(1)	7.6889(1)
β (deg)		90.245(1)	90.246(1)
V (Å^3)		233.466(6)	230.093(7)
Ca	4*e*(*x*,*y*,*z*)		
x		0.9892(4)	0.9893(7)
y		0.0508(3)	0.0489(3)
z		0.2521(4)	0.2486(6)
B (Å^2)		0.74(3)	0.58(4)
T	2*d* (1/2,0,0)		
B (Å^2)		0.63(9)	0.37(3)
W	2*c* (1/2,0,1/2)		
B (Å^2)		0.27(5)	0.35(6)
O1	4*e*(*x*,*y*,*z*)		
x		0.0892(3)	0.0860(4)
y		0.4712(3)	0.4746(4)
z		0.2412(3)	0.2412(3)
B (Å^2)		0.65(3)	0.56(4)
O2	4*e*(*x*,*y*,*z*)		
x		0.7132(3)	0.7133(5)
y		0.3092(4)	0.3057(5)
z		0.0430(2)	0.0430(3)
B (Å^2)		0.58(3)	0.48(4)
O3	4*e*(*x*,*y*,*z*)		
x		0.1884(3)	0.1931(5)
y		0.2174(3)	0.2162(5)
z		0.9504(2)	0.9534(4)
B (Å^2)		0.63(3)	0.61(4)
Reliability factors			
R_p(%)		3.65	3.22
R_{wp}(%)		4.63	4.04
R_{exp}(%)		4.03	3.55
χ^2		1.32	1.29
R_I(%)		3.84	5.02

represent the magnetic moments per Co^{2+} or Ni^{2+} ions in the ordered states and are in both cases in excellent agreement with the spin-only contribution of $3\mu_B$/atom for high spin $Co^{2+}(t_{2g}^5e_g^2)$ or $2\mu_B$/atom for high spin $Ni^{2+}(t_{2g}^6e_g^2)$. The goodness of the fit between the observed and calculated NPD patterns at T = 2 K are illustrated in Figures 6a and 6b.

Discussion

The structure of the monoclinically distorted Ca_2TWO_6 (T = Co, Ni) perovskite contains three inequivalent oxygen atoms, the positions of which cannot be very accurately determined by XRD diffraction as strong pseudo-symmetry is present in the patterns. Probably for this reason, this material had previously been described as orthorhombic [11]. An NPD study was essential to investigate the subtle structural features of this perovskite, neutrons being more sensitive to the oxygen positions.

Several examples of monoclinically distorted, 1 : 1 ordered perovskites have been described in the past,

Table 2. Main bond distances (Å) and selected angles (°) for monoclinic Ca_2TWO_6 (T = Co, Ni) determined from NPD data at 295 K.

		T = Co	T = Ni
TO_6 Octahedra			
T-	O1(×2)	2.063(2)	2.050(2)
T-	O2(2)	2.103(2)	2.073(3)
T-	O3(×2)	2.114(2)	2.075(3)
⟨T-O⟩		2.093(2)	2.066(3)
WO_6 Octahedra			
W-	O1(×2)	1.927(2)	1.915(3)
W-	O2(×2)	1.915(2)	1.916(3)
W-	O3(×2)	1.919(2)	1.921(3)
⟨T-O⟩		1.920(2)	1.919(3)
B-O1-	W (x2)	150.34(9)	151.6(1)
B-O2-	W (x2)	151.12(8)	151.7(1)
B-O3-	W (x2)	149.50(7)	150.9(1)
CaO_9 Polyhedra			
Ca-	O1	2.409(2)	2.415(3)
Ca-	O1	3.169(3)	3.138(4)
Ca-	O1	2.330(3)	2.333(4)
Ca-	O2	2.627(3)	2.593(5)
Ca-	O2	2.353(3)	2.366(5)
Ca-	O2	2.664(3)	2.686(5)
Ca-	O3	2.733(3)	2.692(5)
Ca-	O3	2.587(3)	2.599(5)
Ca-	O3	2.365(3)	2.351(5)
$\langle Ca\text{-}O\rangle_{8\,short}$		2.509(3)	2.504(5)

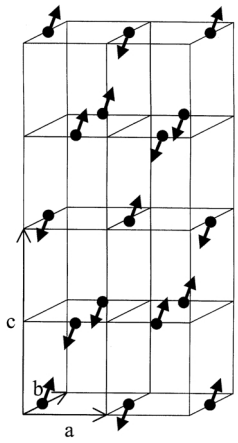

Fig. 4. Schematic view of the magnetic structure of Ca_2CoWO_6. The chemical unit cell is doubled along *x* and *z*. Only Co ions and their magnetic moments (oriented along (011 directions) are represented).

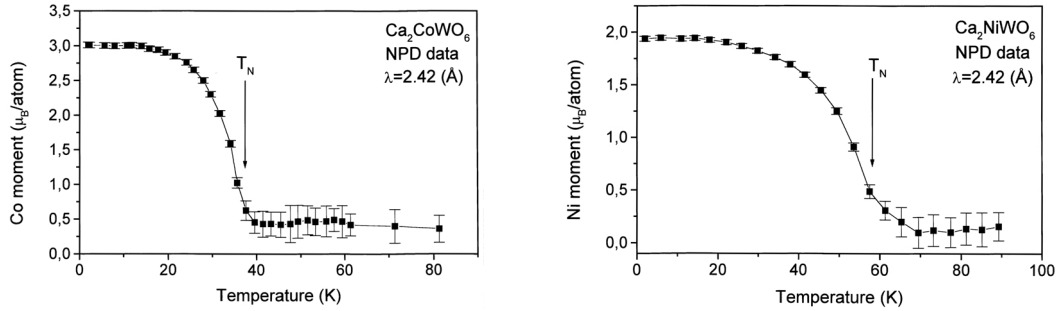

Fig. 5. Thermal evolution of the ordered magnetic moments on T positions refined from NPD data for T = Co (left); T = Ni (right).

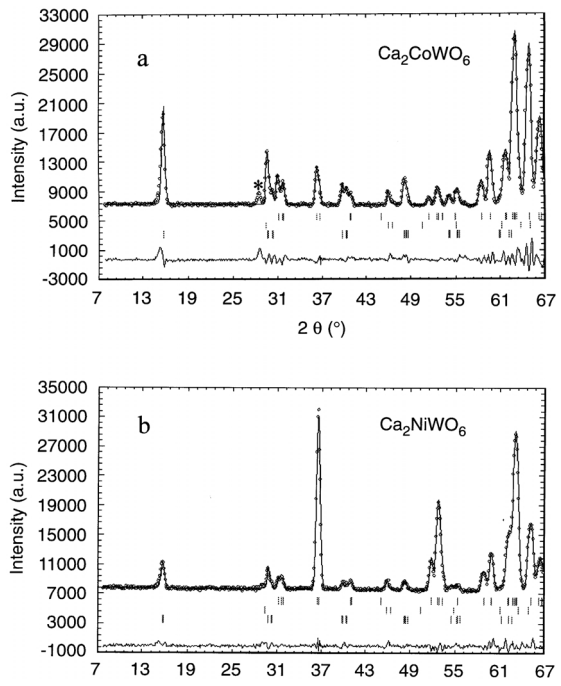

Fig. 6. Observed (crosses), calculated (full line) and difference (bottom) NPD Rietveld profiles for (a) Ca_2CoWO_6 and (b) Ca_2NiWO_6 at 2 K. Vertical lines correspond to the Bragg positions for the crystallographic phase (top) and magnetic phase (bottom). The star corresponds to a reflection from the cryostat.

for instance Nd_2MgTiO_6 [16], Ca_2FeMoO_6 [17], Sr_2MnWO_6, Ca_2MnWO_6, and Sr_2MnMoO_6 [18]. In all cases the compounds crystallize in the space group $P2_1/n$, with $\mathbf{a} \approx \mathbf{b} \approx \sqrt{2}\mathbf{a}_0$ and $\mathbf{c} \approx 2\mathbf{a}_0$, and they show long range ordering between the two different cations placed at the B positions of the A$_2$B'B"O$_6$ perovskite structure. The driving force for the B', B" ordering is the charge difference between both kinds of cations, for instance Mg^{2+} and Ti^{4+} in Nd_2MgTiO_6, or Mn^{2+} and W^{6+} in Sr_2MnWO_6. It is remarkable that all of these compounds show an extraordinarily high pseudo-orthorhombic character as far as unit-cell dimensions are concerned: β angles are very close to 90°, *e.g.* β = 89.969(8)° for Ca_2FeMoO_6 [17]. However, the internal symmetry is monoclinic, as shown from neutron diffraction refinements [16–18]. This is also the case for Ca_2TWO_6 (T = Co, Ni), which are also strongly pseudo-orthorhombic, but show a good and unique convergence in the $P2_1/n$ setting during the refinement of NPD data.

In Table 2 we notice that CoO_6 and NiO_6 octahedra are slightly larger than WO_6 octahedra, in agreement with the difference in ionic radii [15]. The average T–O bond-lengths at RT compare well with the expected values calculated as ionic radii sums [15] for T = Co, ⟨Co–O⟩: 2.093(2) Å (calc. 2.145 Å); ⟨W–O⟩: 1.920(2) Å (calc. 2.00 Å); for T = Ni, ⟨Ni–O⟩: 2.066(3) Å (calc. 2.090 Å); ⟨W–O⟩: 1.919(3) Å (calc. 2.00 Å).

In order to get some insight into the oxidation states distributions, we carried out a series of bond-valence calculations by means of the Brown model [19,20]. This model assumes that the valence of a given cation is shared between the chemical bonds of the first coordination sphere. It defines a phenomenological relationship between the formal valence of a bond and the corresponding bond lengths. Bond valences are calculated with the formula $v_{ij} = \exp[(R_{ij} - d_{ij})/0.37]$, where R_{ij} is the bond-valence parameter and d_{ij} is the anion-cation bond length. The valence of the atom i (V_i) is then calculated as $\sum v_{ij}$. In Ca_2CoWO_6, the calculated valences for Ca, Co, and W are 2.00, 2.03, and 5.95 respectively; in Ca_2NiWO_6, the calculated valences for Ca, Ni, and W are 2.02, 1.98, and 5.96 re-

spectively. From these values the electronic configuration for these compounds at 298 K are $Co^{2+}(3d^7)$-$W^{6+}(5d^0)$, $Ni^{2+}(3d^8)$-$W^{6+}(5d^0)$ respectively, which is in good agreement with the results of the magnetic structure determination at 2 K. These electronic configurations, excluding the presence of a mixed valence at Co(Ni) atoms and implying an oxidation state +6 for W cations, account for the electrical insulating behavior and color of the samples.

Conclusions

The study of the crystal structure of the double perovskites Ca_2TWO_6 (T = Co, Ni) from neutron powder diffraction data allowed us to establish that these oxides have a room temperature monoclinic structure, space group $P2_1/n$. These compounds experience a low-temperature antiferromagnetic ordering; the magnetic structure is defined by the propagation vector $\mathbf{k} = (1/2, 0, 1/2)$. It seems clear that Co and Ni ions adopt an oxidation state +2, in a high spin configuration.

Acknowledgements

We thank the financial support of CICyT to the project MAT2001-0539, and we are grateful to ILL for making all facilities available.

[1] K. Chahara, T. Ohno, M. Kasai, Y. Kozono, Appl. Phys. Lett. **63**, 1990 (1993).
[2] S. Jin, H. M. O'Bryan, T. H. Tiefel, M. Mc. Cormack, W. W. Rhodes, Appl. Phys. Lett. **66**, 382 (1995).
[3] C. N. R. Rao, B. Raveau (eds.): Colossal magnetoresistance and other related properties in 3d oxides, World Scientific, Singapore (1998).
[4] M. T. Anderson, K. B. Green Wood, G. A. Taylor, K. R. Poeppelmeier, Prog. Solid State Chem. **22**, 197 (1993).
[5] F. S. Galasso, F. C. Douglas, R. Kasper, J. Chem. Phys. **44**, 1672 (1966).
[6] K. I. Kobayaski, T. Kimura, H. Sawadw, K. Terakura, Y. Tokura, Nature **395**, 677 (1998).
[7] K.I. Kobayaski, T. Kimura, H. Sawadw, K. Terakura, Y. Tokura, Phys. Rev. Lett. **59**, 11159 (1999).
[8] J. Golapakrishnan, A. Chattopadhyay, S. B. Ogale, T. Venkatesan, R. L. Greene, A. J. Millis, K. Ramesha, B. Hannoyer, G. Marest, Phys. Rev. B **62**, 9538 (2000).
[9] B. García-Landa, C. Ritter, M. R. Ibarra, J. Blasco, P. A. Algarabel, R. Mahendiran, J. García, Solid State Común. **110**, 435 (1999).
[10] T. H. Kim, M. Mehara, S. W. Cheong, S. Lee, Appl. Phys. Lett. **74**, 1737 (1999).
[11] G. Blasse, J. Inorg. Nucl. Chem. **27**, 993 (1965).
[12] G. Blasse, Proc. Int. Conf. Mag. Notthingham 1964, p. 350, Inst. Phys. London (1965).
[13] J. Rodríguez-Carvajal, Physica B (Amsterdam) **192**, 55 (1993).
[14] P. M. Woodward, Acta Crystallogr. B **53**, 32 (1997).
[15] R. D. Shannon, Acta Crystallogr. Sect. A **32**, 751 (1976).
[16] W. A. Groen, F. P. F. Van Berkel, D. J. W. Idjo, Acta Crystallogr. C **42**, 1472 (1986).
[17] J. A. Alonso, M. T. Casais, M. J. Martínez-Lope, J. L. Martínez, P. Velasco, A. Muñoz, M. T. Fernández-Díaz, Chem. Mat. **12**, 161 (2000).
[18] A. Muñoz, J. A. Alonso, M. T. Casais, M. J. Martínez-Lope, M. T. Fernández-Díaz, J. Phys. Cond. Mat. **14**, 8817 (2002).
[19] I. D. Brown, in M. O'Keefe, A. Navrotsky (eds): Structure and Bonding in Crystals, Vol 2, p. 1, Academic Press, New York (1981).
[20] N. E. Brese, M. O'Keefe, Acta Crystallogr. Sect. B **47**, 192 (1991).